EJN European Journal of Neuroscience

FENS Federation of European Neuroscience Societies

European Journal of Neuroscience, pp. 1–15, 2015 doi:10.1111/ejn.12904

Electrophysiological evidence of alterations to the nucleus accumbens and dorsolateral striatum during chronic cocaine self-administration

Kevin R. Coffey,* David J. Barker,* Nick Gayliard, Julianna M. Kulik, Anthony P. Pawlak, Joshua P. Stamos and Mark O. West

Department of Psychology, Rutgers University, Piscataway, NJ 08854, USA

Keywords: addiction, basal ganglia, single-unit, stimulant

Abstract

As drug use becomes chronic, aberrant striatal processing contributes to the development of perseverative drug-taking behaviors. Two particular portions of the striatum, the nucleus accumbens (NAc) and the dorsolateral striatum (DLS), are known to undergo neurobiological changes from acute to chronic drug use. However, little is known about the exact progression of changes in functional striatal processing as drug intake persists. We sampled single-unit activity in the NAc and DLS throughout 24 daily sessions of chronic long-access cocaine self-administration, and longitudinally tracked firing rates (FR) specifically during the operant response, an upward vertical head movement. A total of 103 neurons were held longitudinally and immunohistochemically localised to either NAc Medial Shell (n = 29), NAc Core (n = 30), or DLS (n = 54). We modeled changes representative of each category as a whole. Results demonstrated that FRs of DLS Head Movement neurons were significantly increased relative to baseline during all sessions, while FRs of DLS Uncategorised neurons were significantly reduced relative to baseline during all sessions. NAc Shell neurons' FRs were also significantly decreased relative to baseline during all sessions while FRs of NAc Core neurons were reduced relative to baseline only during training days 1–18 but were not significantly reduced on the remaining sessions (19–24). The data suggest that all striatal subregions show changes in FR during the operant response relative to baseline, but longitudinal changes in response firing patterns were observed only in the NAc Core, suggesting that this region is particularly susceptible to plastic changes induced by abused drugs.

Introduction

The striatum is the receiving area of the basal ganglia, processing inputs from cortex, thalamus, limbic structures such as the amygdala, and midbrain dopamine neurons (Zahm & Heimer, 1988, 1990; Parent, 1990; Brog *et al.*, 1993; Wright *et al.*, 1996; Usuda *et al.*, 1998; Haber *et al.*, 2000). Signals processed within the striatum project sequentially to the globus pallidus and subthalamic nucleus and then on to premotor areas where they are capable of affecting behavioral output. Accordingly, it has been proposed that these cortex–striatum–thalamus–cortex re-entrant loops process limbic and sensorimotor information in order to monitor ongoing behaviors as well as to affect future action selection (Nauta *et al.*, 1978; Alexander *et al.*, 1986).

It is thought that, as drug use transitions to chronic abuse, aberrant striatal processing contributes to the development of perseverative drug-taking (Robbins & Everitt, 2002; Gerdeman *et al.*, 2003; Volkow *et al.*, 2006; Belin & Everitt, 2008; Thomas *et al.*, 2008) that persists despite adverse consequences (Tiffany, 1990; Feltenstein & See, 2008; Root *et al.*, 2009; Marchant *et al.*, 2013). These changes are linked to interactions between abused drugs and dopaminergic transmission in the striatum. Several studies suggest that two portions of the striatum, the nucleus accumbens (NAc) and the dorsolateral striatum (DLS), undergo neurobiological changes as drug use progresses from acute to chronic (Letchworth *et al.*, 2001; Nader *et al.*, 2002; Macey *et al.*, 2004; Porrino *et al.*, 2004; Hanlon *et al.*, 2009; Willuhn *et al.*, 2014). Despite knowledge of the somatotopic organisation of the DLS (Crutcher & Delong, 1984; Carelli & West, 1991; Brown, 1992; Mittler *et al.*, 1994; Brown & Sharp, 1995; Cho & West, 1997), and that sensorimotor processing is altered during the course of chronic cocaine use (Hanlon *et al.*, 2009), little is known about changes in phasic processing of individual DLS neurons during this progression, making it difficult to predict how they might contribute to future drug-taking or relapse behaviors.

The goal of the present study was to electrophysiologically record single-unit activity in the NAc and DLS throughout chronic long-access cocaine self-administration (Ahmed & Koob, 1998) and longitudinally track activity specifically during the operant response. Recording wires were divided into four groups based first on histochemical localisation within the DLS (François *et al.*, 1994) or to

Correspondence: Mark O. West, as above.
E-mail: markwest@rutgers.edu

*Co-first Authors.

Received 5 December 2014, accepted 25 March 2015

either the Core or Shell subregions of the NAc (Meredith *et al.*, 1996) using antibodies against Calbindin D28k. Next, because many DLS neurons show somatic sensorimotor firing properties, we further characterised them via a sensorimotor examination prior to training (Carelli & West, 1991). DLS neurons that fired selectively during vertical head movement (Tang *et al.*, 2007) were separated from DLS neurons that did not explicitly exhibit a sensorimotor correlate. Animals were trained to perform a vertical head movement reinforced by cocaine in order to engage DLS Head Movement neurons in processing the operant drug-taking response. Population activity for striatum as a whole, as well as each NAc and DLS subgroup, were examined during the operant response, and changes in response-related firing patterns were modeled longitudinally.

Materials and methods

Subjects and surgery

Details of the general surgical procedure have been described previously (Root *et al.*, 2013). Adult male Long–Evans rats (Charles River, Wilmington, MA, USA) were implanted with a catheter in the right jugular vein and a 16-microwire array (2 × 8; Micro-Probes, Gaithersburg, MD, USA) targeting either the right DLS (n = 19) or right NAc (n = 21). Arrays were implanted through a rectangular craniotomy with the following corners (ML mm, AP mm) relative to bregma – DLS [(2.8, 2.5) (3.4, 2.6) (3.4, −0.5) (4.0, −0.4)], NAc [(0.6, 0.5) (1.8, 0.5) (0.6, 3.0) (1.8, 3.0)]. Arrays were constructed from 50-μm stainless steel microwires quad coated in Teflon® insulation. Arrays targeting the DLS were constructed with 300 μm spacing between rows and columns, while those targeting the NAc were constructed with 250 μm between rows and 750 μm between columns. Arrays were lowered using a motorised stereotaxic device (Coffey *et al.*, 2013) at a rate of 200 μm/min to a depth of 3.9 mm below the surface of the skull for the DLS or 6.7 mm below the skull surface for the NAc. A stainless-steel ground wire (0.25 mm diameter) with 5 mm of exposed wire was also implanted contralateral to the microwire array 5.5 mm ventral to the skull surface. Recovery took place in individual Plexiglas self-administration chambers, which served as the animals' home cages for the duration of the experiment. Animals were provided with food after each self-administration session to maintain body weight between 310 and 350 g (~ 85% of free-feeding weight as estimated based on growth curves from Charles River). Experiments were performed in compliance with the Guide for the Care and Use of Laboratory Animals (NIH, 1985; Publication 865–23) and have been approved by the Institutional Animal Care and Use Committee, Rutgers University (Institute of Laboratory Animal Resources, 1985).

Body exam

Neurons in the DLS are responsive to somatosensory and/or motor activity of single body parts (Crutcher & Delong, 1984; Alexander & DeLong, 1985; Liles & Updyke, 1985; West *et al.*, 1990; Carelli & West, 1991; Mittler *et al.*, 1994; Cho & West, 1997). Prior to self-administration, animals with arrays targeting the DLS underwent an exam of the anterior body parts (omitting hindlimbs and tail). The purpose was to select DLS neurons that were targeted for this study (i.e., those that were related specifically to vertical head movement). Neuronal signals were amplified 7000× and online-discriminated spiking activity was played through a pair of headphones to assess whether body part stimulation and/or manipulation resulted in changes in firing rate (FR). Animals were trained to remain entirely still, resulting in low baseline FRs of DLS neurons. Each neuron was then tested for responsiveness to experimenter manipulation and/or cutaneous stimulation of the following regions – ipsilateral and contralateral forelimbs, vibrissae and shoulders, as well as the head, neck, snout and chin. For experimenter manipulation, each body part was physically moved up, down, left and right while the rest of the body remained motionless. Neurons were considered to process movement if discharges occurred during single body part manipulation in the absence of any other body part movements. For cutaneous stimulation, a hand-held probe (2 mm diam.) calibrated to deliver 1–2 g of force was used. Each body part was tapped with the probe and the fur or skin was gently rubbed with light stroking movements. Neurons were considered to process cutaneous touch if discharges occurred during single body part stimulation in the absence of discernible movements. This approach unambiguously assigned each responsive neuron to a particular category.

Head Movement neurons were defined as those that responded to cutaneous stimulation of the head or neck (other than the face) or fired during spontaneous or experimenter-induced head movements. Neurons that responded to other specific body parts were excluded from the present study because the automated measurement of movements (see next section) was selective for head/neck and could not monitor other body parts. For example, vibrissae neurons were excluded because, although vibrissae contacted the walls of the photocell corner during the operant response, we did not measure activity of the vibrissae. Any neuron not assigned to a particular category described above (i.e., unresponsive during the sensorimotor exam) was included as an Uncategorised neuron in this study.

Procedures and experimental apparatus

Detailed descriptions of the experimental apparatus have been published previously (Root *et al.*, 2013; Barker *et al.*, 2014). The photocell device used for operant responding (Fig. 1) consisted of a series of six infrared-emitting diodes capable of transistor–transistor logic (HOA-6299; Honeywell, Morristown, NJ, USA), which were positioned along a 50° arc over 69 mm. Each photocell emitted a beam with a 5.59-mm diameter and an 880-nm wavelength. The photocell apparatus was attached to the outside of the back left corner of the operant chamber with the lowest photocell positioned ~ 13 mm from the floor of the chamber. The lowest photocell will be referred to as photocell one, with incrementing photocells referred to as two through six. During shaping and training, a 750 Hz tone (70 dB) was presented at the completion of the operant response (0.5 s duration) using a custom tone generator (M. B. Turnkey Design, Hillsborough, NJ, USA). All experimental apparatus were controlled by a PC running MED-Associates hardware and software (St Albans, VT, USA). During hours when self-administration sessions were not in effect a Plexiglas block (50.8 × 50.8 × 152.4 mm) was inserted into the corner to block the photocell device and prevent extinction learning.

The operant response and schedule of reinforcement in this study were custom-designed specifically to improve the quality of data collected in this experiment. The vertical head movement operant response was chosen because (i) it has a discrete beginning and end sandwiched between approach and retreat from the corner (Root *et al.*, 2013), unlike lever pressing, which can include rapid movements of many body parts, even locomotion or turning as a rat self-administering cocaine moves rapidly past the lever, and (ii) it has been demonstrated to become habitual with extended training, as employed here (Tang *et al.*, 2007). The vertical head movement operant response is more complex than the traditional lever press so,

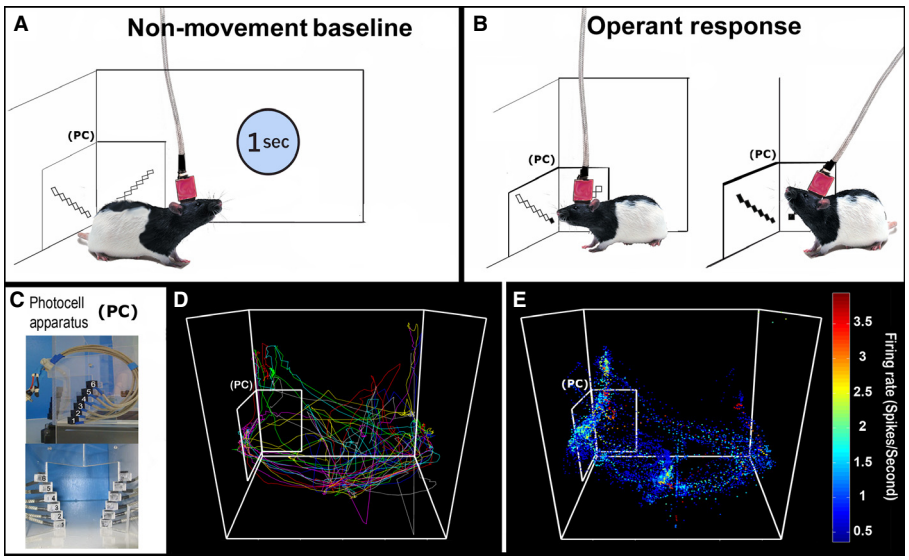

FIG. 1. Video tracking and baseline FR calculation. (A) Each rat's head position was tracked and used to isolate 1-s periods of non-movement. (B) Operant head movements were measured accurately in the corner by a custom photocell device in order to reward vertical head movement responses with cocaine. A criterion head movement (PC2–PC5; < 1 s) produced an infusion. (C) Photographs of the actual photocell device mounted outside the corner of the operant chamber (top) and from the animal's perspective (bottom). (D) An animal's position tracked continuously over 10 trials of a self-administration session, plotted in alternating colors for clarity. (E) Positional data from an entire session overlaid with FR data, used to determine FRs during non-movement only.

to facilitate shaping, the first 3–5 days of self-administration employed a fixed-interval (FI) 10-s schedule of cocaine availability and responses were reinforced with a moderately large (0.24 mg in 0.2 mL) infusion of cocaine administered over 7.5 s. Animals were shaped to make a vertical head movement by reinforcing successive approximations of the movement, starting with a single-photocell break at photocell two. The response requirement was incremented by one photocell after every seven successful responses were performed, until subjects were successfully breaking photocells two through five consecutively in an upward movement < 1 s in duration (termed the 'criterion response').

Once animals performed 40 or more criterion responses during a single session, they progressed from shaping to self-administration training. During each training session subjects were allowed to load-up on an FI 10 s schedule for the first nine infusions. Criterion responses during the load-up period produced a 0.24 mg in 0.2 mL cocaine infusion administered over 7.5 s, allowing animals to rapidly increase drug level. Responses during the load-up phase were removed from analysis in order to remove the effect of rapidly changing pharmacology from our measure of response-related activity. Following the load-up period, animals progressed into a pseudo-random variable interval (VI) 30-s schedule for maintenance responding. Reinforced responses 10–19 produced a 0.12 mg/0.1 mL infusion over 3.75 s. From infusion 20 onward, animals received the maintenance dose of 0.06 mg in 0.05 mL delivered over 1.875 s. This change in schedule was designed to yield two benefits. First, the unsignaled VI schedule removed the effect of anticipation as the animals could not predict which responses were reinforced, allowing us to analyse all operant responses together. Second, the low maintenance dose caused animals to respond more often to maintain a stable drug level, and the variable timeouts allowed for many unreinforced responses. This maximised the number of responses animals made each session, giving us sufficient numbers of matched movements (discussed below) for neural analyses. For both load-up and maintenance, if an animal failed to produce a response within 1 min after the VI 30-s had elapsed, the cocaine availability period ended and a new interval began. Training and shaping lasted a total of 24 sessions on 24 consecutive days and lasted for 6 h each day.

Electrophysiological recordings

Recording procedures and parameters

Single-unit activity was recorded approximately every other day for a period of 24 days. Neural signals from all 16 microwires were amplified at the level of the headstage using a harness with four quad-channel operational amplifiers (MB Turnkey Design, Hillsborough, NJ, USA). Each harness connected to a fluid and electrical swivel (Plastics One Inc., Roanoke, VA, USA) through which signals were fed to a preamplifier and filter (MB Turnkey Design). The preamplifier differentially amplified (10×) the signal on each recording electrode against another wire on the implanted array that did not display a neuron. The filter then amplified (700×) and band-passed signals between 450 Hz and 10 kHz with a roll off of −1.5 dB per octave below 1 kHz and −6 dB per octave above 11 kHz. Finally, signals were digitised at a 50-kHz sampling frequency and were recorded using DATAWAVE Technologies hardware and software (Longmont, CO, USA). All signals were then stored for offline sorting and analysis. During each session, electrophysiological recordings began concurrently with the start of the self-administration session and terminated at the end of the session. Isolation of individual neural waveforms from background noise was performed offline using SciWorks spike sorting and separation software (DATAWAVE). All waveforms of the putative individual neuron during the entire session (6 h) were displayed in temporal order on a computer-simulated oscilloscope to assess the stability of neural waveforms within session. An inter-spike interval (ISI) histogram was also constructed. If discharges occurred within the first 2 ms in the ISI corresponding to a neuron's natural refractory period, the recording was not considered that of a single neuron and was discarded (Kosobud *et al.*, 1994; Peoples *et al.*, 1999). Neurons

exhibiting signal-to-noise ratios < 2 : 1 were also discarded. Finally, if one wire exhibited two different waveforms (1.7% of recorded cells), a cross-correlogram was constructed for that wire. Using the cross-correlogram, it was determined that two separate neurons were present if spikes occurred within the first two 1-ms bins, representing the refractory period for a single neuron.

Criteria for identifying the same single neuron across sessions

Under circumstances similar to those in the present study, neurons can be recorded longitudinally using microwire arrays (Thompson & Best, 1990; Greenberg & Wilson, 2004; Schmitzer-Torbert *et al.*, 2005; Jackson & Fetz, 2007; Tang *et al.*, 2007, 2009; Tolias *et al.*, 2007; Dickey *et al.*, 2009; Fraser & Schwartz, 2012; Lütcke *et al.*, 2013; McMahon *et al.*, 2014). A key feature of the striatum that facilitates single unit isolation is that medium spiny neurons (MSNs) are homogeneously dispersed (i.e., not layered) and their small soma exhibit single spikes of small amplitude which decay over a short distance. Waveforms of MSNs typically exhibit maximal amplitude (subtracting our typical 50-μV noiseband) of ~ 170 μV. Using Rall (1962) calculation applied to MSNs [i.e., somal diameter of ~ 20 μm and radially symmetric dendrites (the 'closed field' model)], waveform amplitude would decline by 170 μV at a distance of 34 μm and thus be undetectable. Thus, the spikes of one neuron rarely interfere with discriminating the spikes of another. From 1 day to the next, the same wires in a given animal exhibit stable waveform recordings throughout the 6-h session (Peoples *et al.*, 1999; Ghitza *et al.*, 2003 for NAc; Tang *et al.*, 2007 for DLS).

To assert that the same neuron was recorded over sessions in the present study, the following criteria were met: (i) each waveform present throughout the period in question was recorded from the same microwire; (ii) waveforms had similar shapes – the correlation between the average waveforms (average waveform voltages during the spike, sampled at 35 time points at 50 kHz) from one session to the next was > 0.9; (iii) waveforms had similar parameters – the difference in spike height from one session to the next was < 20%, and the difference in peak time from one session to the next was < 0.04 ms; and (iv) alternative explanations were also ruled out using a combination of logical inference (see above paragraph) and modeling of waveform stability using real data, as follows.

Within-wire waveform stability was calculated by determining the total area displaced when overlaying the mean waveform from each session recorded from a single wire. These areas were compared to the expected areas of waveforms from alternative explanations. The most extreme alternative explanation is that each given wire recorded a different striatal neuron on every session. This alternative was modeled by randomly selecting waveforms from different wires for an equal number of sessions as recorded by each given wire. A more conservative alternative explanation is that a unit is lost and a second unit is gained somewhere in training. This alternative was modeled by selecting half of the session's waveforms from a single wire and randomly selecting the other half of the session's waveforms from a different wire. Under the assumption that all waveforms recorded from a single wire belong to a single-unit, we predict minimal waveform area. We also predict greater waveform area when half the waveforms come from a second wire and even greater area when all waveforms are selected from all different wires. Statistical analysis of the difference in area of waveform displacement between real and modeled distributions was accomplished using two-sample Kolmogorov–Smirnov tests.

Analysis of neural data

Behavioral equivalence

The concept of behavioral equivalence (Porrino, 1993) is important for comparing neural measures in awake animals across conditions in order to eliminate sensorimotor differences as a possible alternative explanation of neural results. This is especially important in the present data, as DLS neurons are sensitive to sensorimotor processing and the topographies of observed behaviors can change across learning, potentially affecting FR of both NAc and DLS neurons. Thus, behaviors tracked across longitudinal recordings were analysed using 'matched sets' (Tang *et al.*, 2007, 2009). Matched sets are equivalent motor behaviors observed across sessions. Specifically, similar movements were categorised based on parameters such as movement distance or duration (described below). A movement type was included in the longitudinal analysis when at least five alike movements were observed in a given category on each of four or more sessions. While this technique excludes many unmatched movements from analysis, we believe that analysing behaviorally equivalent data is essential for interpreting longitudinal changes in neural activity.

Response-related firing patterns

To examine firing patterns during the operant response, head movements (Fig. 1) were sorted into 50 unique movement categories. These 50 categories correspond to a combination of ten unique categories of movement start and end positions (movement distance) at five different categories of movement duration (Table 1). In order to effectively match movements across all sessions and maximise sampling of each neuron's FR, categories cover a multitude of movements and not just the 'criterion response' for self-administration behavior.

Specifically, start position was broken into 4 bins starting at photocell (PC) 1 and incrementing by 1 until PC 4, while end position was broken into 4 bins starting at PC 3 and incrementing by 1 until PC 6. Duration consisted of 5 bins starting at 100 ms and incrementing by 180 ms until 1000 ms; note that only movements > 100 ms that contained at least two PC breaks were accepted and many categories at the extremes contained no observations (Table 1). Movements from different sessions that fell into the same category of start position, distance and duration were considered 'matched sets'. In accordance with our previous work, only categories containing at least five movements on every recorded session were considered for analysis (Tang *et al.*, 2007). FRs from matched sets maintained across sessions were compared to baseline FR within each session using the ratio 'ΔFRresponse = (Response FR − Baseline FR)/(Response FR + Baseline FR)'. Change ratios were then examined across sessions.

Calculation of baseline FR

FRs of neurons in the DLS are sensitive to the sensorimotor activity of single body parts; neurons in the NAc have similarly been repeatedly implicated in behaviors that involve some form of motor behavior (e.g., operant responding). Therefore, response-related FR was not compared to the immediately preceding FR, which would have varied with motor behaviors involved in approaching the photocell corner (Root *et al.*, 2013). Instead, movement-free epochs were used to calculate baseline FRs as a control for possible influences of motor behaviors on baseline firing. To determine movement-free epochs, a custom MATLAB script was used to examine subjects' video tracked coordinates across the entire session and extract moments when rats exhibited no movement for a period of

TABLE 1. Movement categories and behavioral matching

	Average neural firing rates (spikes/s) Duration start–end (ms)				
Photocell	100–280	280–460	460–640	640–820	820–1000
Early (e.g. Day 1)					
1:3	2.6*	NA	NA	NA	NA
1:4	3.2*	2.3*	2.8	2.6*	NA
1:5	NA	2.6*	2.6*	NA	1.9*
1:6	NA	2.2*	2.6	2.6*	2.6*
2:4	3.6*	2.6*	2.3*	1.6	NA
2:5	3.2	2.9*	2.3*	1.4*	NA
2:6	NA	NA	2.9*	2.6*	1.5*
3:5	4.6*	2.8*	2.6*	2.2*	NA
3:6	2.1*	1.5*	NA	NA	NA
4:6	2.2	2.6*	NA	NA	NA
Middle (e.g. Day 12)					
1:3	1.6*	2.6	NA	NA	NA
1:4	3.1*	2.7*	NA	2.3*	2.2
1:5	NA	2.6*	2.3*	3.2	1.4*
1:6	NA	6.3*	2.6	2.6*	2.7*
2:4	3.6*	2.6*	2.5*	NA	NA
2:5	NA	1.4*	2.3*	1.4*	NA
2:6	NA	NA	1.3*	2.6*	3.2*
3:5	4.6*	2.6*	2.6*	1.5*	NA
3:6	2.1*	2.1*	2.7	NA	2.7
4:6	2.2	3.8*	2.2	NA	NA
Late (e.g. Day 24)					
1:3	2.6*	NA	NA	NA	NA
1:4	3.2*	2.3*	NA	2.6*	NA
1:5	NA	2.6*	2.4*	1.5	1.4*
1:6	NA	2.2*	NA	1.8*	2.2*
2:4	3.6*	2.6*	2.6*	1.6	NA
2:5	3.2	1.9*	2.3*	1.4*	NA
2:6	1.7	NA	1.5*	2.6*	4.2*
3:5	4.6*	1.4*	2.6*	NA	NA
3:6	2.1*	2.2*	2.6	NA	1.6
4:6	NA	3.6*	NA	NA	NA

Head movements were sorted into 50 unique movement categories, corresponding to a combination of ten categories of movement start and end positions and five categories of movement duration. Categories are displayed in tables for three example time points. Movements from different sessions that fell into the same category of start position, distance and duration were considered a 'matched set'. In accordance with our previous work, only categories containing at least five movements on every recorded session were considered for analysis. Firing rates marked with * belong to categories with at least 5 movements on at least 4 sessions and were therefore included in the final analyses.

1 s (tracked point deviated < 5.03 mm; Fig. 1). The number of discharges per second during each period was used to calculate average FR during all movement-free intervals. FR during movement-free periods will henceforth be referred to as 'baseline FR'. Comparisons between baseline FR and other methods for calculating an FR baseline (i.e., utilising a pre-node period or a scrambled or randomly sampled baseline) revealed that all measures of baseline FR were highly correlated (all $r \geq 0.90$). Thus, while the movement-free baseline was specifically chosen as a control for the behaviors of interest, it was similar to all aforementioned canonical baseline measures.

Histological procedures

Following self-administration training, animals were given an overdose of sodium pentobarbital (150–200 mg/kg). Anodal current (50 μA for 3 s) was passed through each microwire to produce a small lesion for localising each microwire tip. Animals were then transcardially perfused with 0.9% phosphate buffered (PB) saline followed by 4% paraformaldehyde. The brain was removed and post-fixed in 4% paraformaldehyde before transitioning into a cryoprotectant solution of 30% sucrose in PB. A microtome was used to section brains into 50-μm-thick coronal slices through the extent of the NAc and DLS.

Immunohistochemistry was carried out under gentle agitation using a horizontal rotator (Laboratory-Line, Fisher, Pittsburgh, PA, USA). Free-floating sections were washed for 10 min three times (3 × 10 m) in PB, and then were rinsed for 15 min in a 0.3% H_2O_2 solution to quench endogenous peroxidase. Sections were then washed in PB for 3 × 10 min before treatment with blocking solution (4% bovine albumin + 0.3% triton X-100 in PB) for 1 h. Sections were subsequently transferred into the primary antibody solution containing anti-calbindin d28k diluted in blocking solution (Immunostar, Inc., Hudson, WI, USA) at a 1 : 5000 ratio for a minimum of 16 h at 4 °C (gently agitated and refrigerated overnight). Following incubation in the primary antibody, sections were rinsed for 3 × 10 min in PB and transferred to a solution containing biotinylated secondary antibody against rabbit immunoglobulin (1 : 200 dilution; Vector Laboratories Inc., Burlingame, CA, USA) in blocking solution for 1 h at room temperature. Again, sections were rinsed in PB (3 × 10 min) prior to incubation with a solution containing avidin-biotinylated horseradish peroxidase complex (ABC kit; Vector Laboratories Inc.) for 1 h. Finally, sections were rinsed in PB (3 × 10 min) before developing the peroxidase reaction with 0.05% 3,3-diaminobenzide-4 HCl (DAB; Vector laboratories Inc.) and 0.003% H_20_2 for 2–5 min.

Individual slices were mounted onto gelatin-coated slides before incubation in a solution of 5% potassium ferrocyanide and 10% HCl to stain iron deposits left at the location of the lesioned microwire tip. Sections were then rinsed (3 × 1 min) in water to neutralise the reaction. Processed sections were then dehydrated through a graded series of ETOH before being transferred into a primary xylene solution for 2 min and then a second xylene solution while slides were cover slipped with Permount (Fisher, Pittsburgh, PA, USA) and left to dry for 48 h.

Statistical analyses

Analysis of behavioral data

Behavioral variables (criterion head movements, velocity, etc.) were analysed as a function of training day using repeated-measures ANOVAS (SPSS/PASW 18, Chicago, IL, USA). The alpha criterion for all tests was 0.05. For any repeated-measures ANOVA where sphericity could not be assumed, a Huynh–Felt correction was applied. Corrected contrast tests (Holm–Bonferroni) were used to determine where behavior stabilised by comparing each day in the first 2 weeks to the last week of self-administration.

Analysis of neural data

Analyses of the neural firing patterns for the above-mentioned behavioral events were conducted using a linear mixed model (also known as a hierarchical linear model; Raudenbush & Bryk, 2002) in SAS PROC GLIMMIX (SAS Institute Inc., Cary, NC, USA). All models included (from 24 self-administration sessions) a maximum of 12 continuously modeled recording sessions and four categorical levels of neuron type (i.e., NAc Core, NAc Shell, DLS Head-Movement and DLS Uncategorised). The outcome variable for the model was the ΔFR response change score (described above) for matched head movements during each individual session.

Previous experiments have shown subregional differences in striatal function during repeated stimulant administrations (Porrino *et al.*, 2004; Willuhn *et al.*, 2014). Accordingly, *post hoc* comparisons between means for each model (i.e., *post hoc t*-tests) were performed and Sidak–Holm-adjusted to control for inflated Type I error via an inflated familywise error rate. Also, the present experiment is predicated on previous evidence suggesting that changes in striatal function occur over time when stimulants are repeatedly administered (see Introduction). Accordingly, *post hoc* comparisons for change scores were made at the level of each recording session and designed to examine whether each value differed from a value of zero, representing no change. For all tests alpha was set to 0.05.

Results

Histology

Sections were processed for anti-calbindin d28k immunohistochemistry, which has been shown to differentiate the NAc Core and Shell (Fudge & Haber, 2002) and the sensorimotor DLS from other parts of dorsal striatum (Brown *et al.* 1998). A total of 59 longitudinally held neurons were localised to NAc subregions and of the 205 units localised to the DLS, 54 met the criteria for inclusion in this study (Fig. 2). Among NAc neurons, 29 of the recorded cells were verified within the boundaries of the NAc Medial Shell, while the remaining 30 were verified to have been recorded from the NAc Core. Body exams for neurons verified to have been recorded from the DLS revealed that 27 microwires recorded activity of Head Movement neurons. Another 27 DLS neurons did not respond to stimulation of any tested body part and were therefore designated as Uncategorised.

Behavior

Preliminary statistical analyses of behavior (not shown) revealed no differences between animals implanted with microwires in the DLS versus those implanted with microwires into the NAc. Therefore, behavioral data were collapsed. Animals significantly increased the number of criterion head movements emitted over sessions

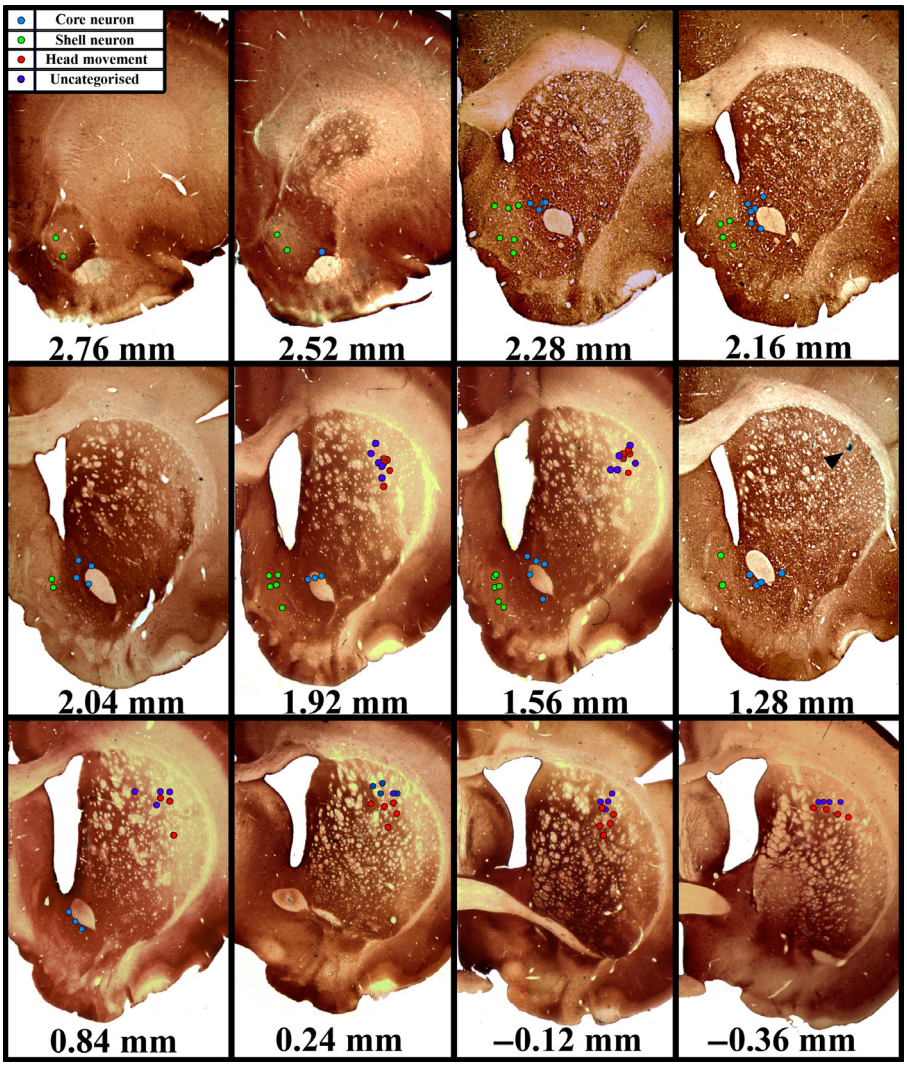

FIG. 2. Histochemical verification of microwire placement. Representative coronal slices through the rat striatum. All slices were processed for anti-calbindin d28-k, which histochemically differentiates the NAc Shell and Core as well as the DLS from the dorsomedial and ventral striatum. All NAc Shell and DLS microwires were localised to calbindin d28k-immunonegative regions. All NAc Core neurons were localised to calbindin d28k-immunopositive regions. Arrow head in 1.28-mm section shows an actual lesion left by a microwire tip.

($F_{20,780}$ = 12.33, P < 0.001; Fig. 3A). Criterion movements became stable from session 5 onwards (sessions 1–4 – all $F_{1,39}$ > 11.7, P < 0.05; Fig. 3A). The increase in the number of criterion head movements over sessions corresponded to a significant increase in drug consumption over sessions ($F_{20,780}$ = 18.27, P < 0.001; Fig. 3B). Increases in drug consumption became stable from session 8 onwards (sessions 1–7 – all $F_{1,39}$ > 4.1, P < 0.05; Fig. 3B).

Behavioral data also demonstrated that operant -head movements were learned over time. This was demonstrated by a significant increase in animals' average starting positions for vertical head movement over sessions ($F_{20,780}$ = 6.50, P < 0.001; Fig. 3C), which stabilised from session 4 onwards (sessions 1–3 – all $F_{1,39}$ > 8.6, P < 0.05; Fig. 3C), as well as a significant increase in movement velocity over sessions ($F_{20,780}$ = 4.35, P < 0.001; Fig. 3D), which did not appear to stabilise. While not required, the change in movement start position demonstrated that animals gradually restricted their movements to the criterion range. Increases in movement velocity also represented non-required increases in movement efficiency. Notably, these types of changes in movement efficiency are consistent with our previous observations and with descriptions of behaviors that become skilled and automatic (Tiffany, 1990; Root *et al.*, 2013).

Extracellular recordings

Stability analysis

Waveform variance across sessions for individual wires was significantly smaller than the variance expected from the alternative explanations. Modeling the assumption that a neuron was lost and that a second neuron was gained across days, waveforms would be significantly more varied than was actually observed (D_{113} = 0.419, P < 0.001; Fig. 4, blue vs. yellow). Modeling the assumption that a neuron was lost and a new neuron was recorded every day, waveforms exhibited even greater variance than those observed from wires meeting the stability criteria (D_{113} = 0.694, P < 0.001; Fig. 4, blue vs. red). Both the known morphology of the striatum and models of alternative explanations support the interpretation that signals from the same striatal neurons were held across sessions. Therefore, stable waveforms recorded on the same single wire across sessions were considered to belong to a single neuron.

Baseline FR

Baseline FRs did not significantly differ between subregions ($F_{3,786}$ = 1.5, P > 0.05, N.S.), nor did they change across recording

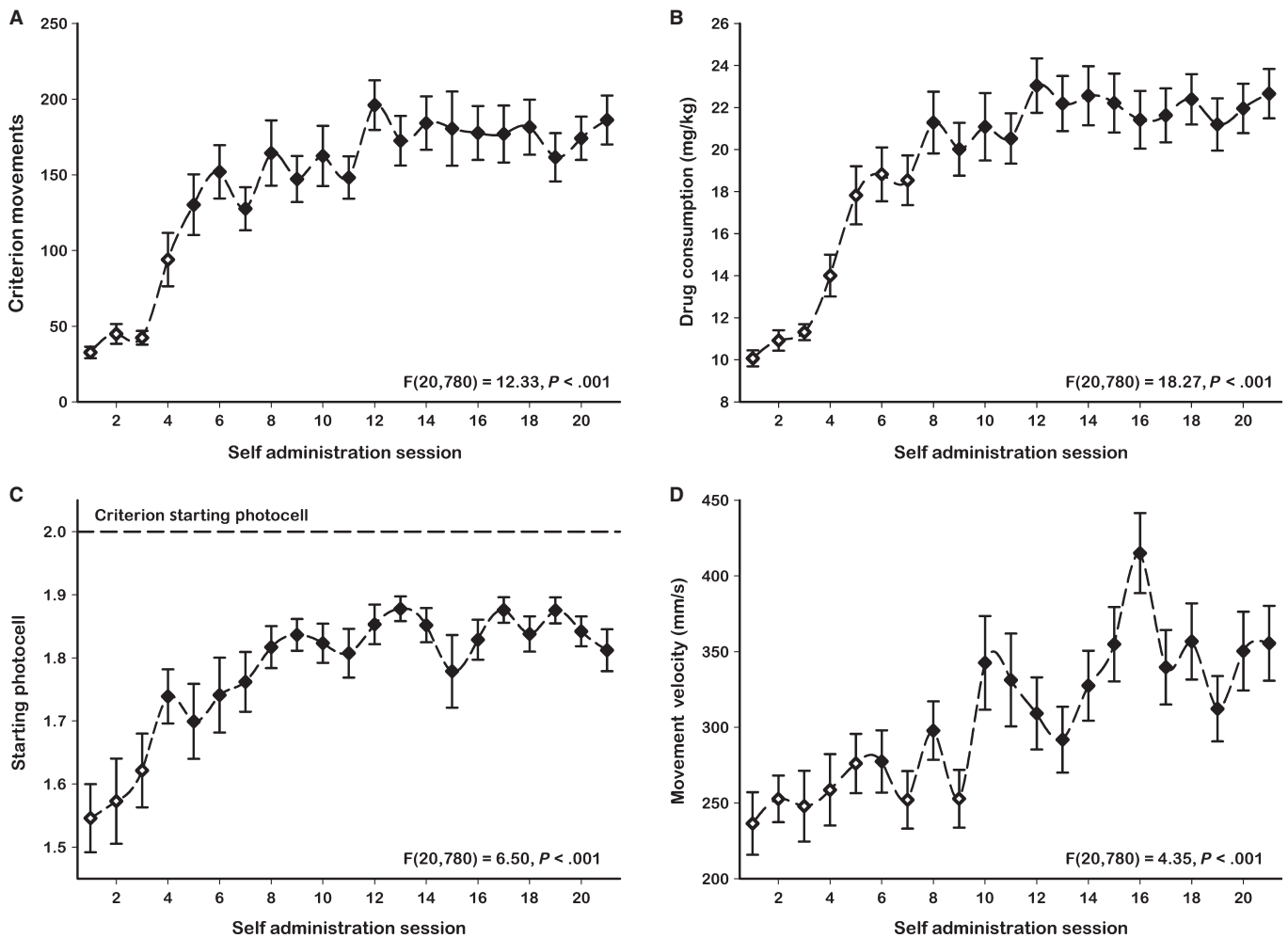

FIG. 3. Behavioral changes over time. (A) Animals significantly increased criterion head movements ($F_{20,780}$ = 6.5, P < 0.001) and (B) increased drug consumption ($F_{20,780}$ = 18.27, P < 0.001) across days. (C) Animals also learned to begin their head movements closer to the required start position ($F_{20,780}$ = 6.5, P < 0.001) and (D) significantly increased their movement velocity ($F_{20,780}$ = 4.35, P < 0.05) across days. Hollow markers represent sessions in which that particular measure was significantly different (corrected contrast tests, P < 0.05) from that measure during the last week of training.

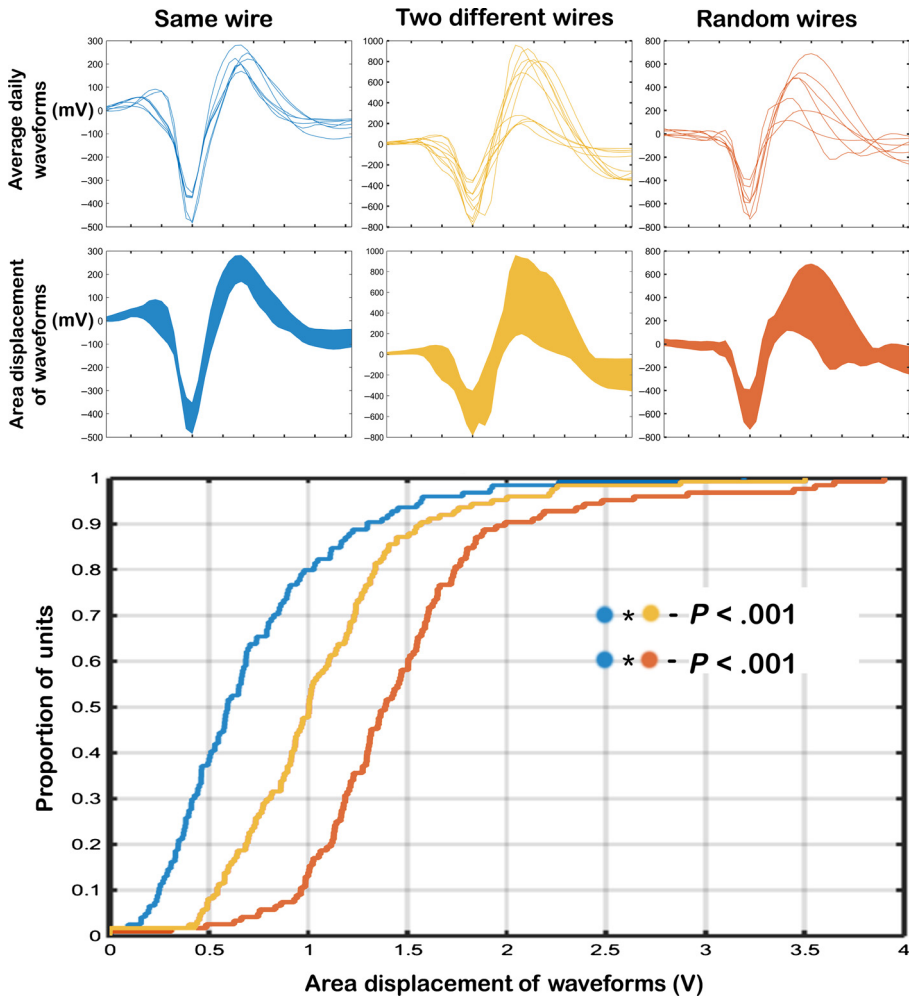

FIG. 4. Waveform stability models. (Top) An example of total waveform variance across days is shown for a single wire (left), the combination of two wires (center) and for a combination of random wires (right). (Bottom) Cumulative distribution functions for waveform variance when data were taken from individual wires (left), two different wires (center) or random wires (right). Waveform variance on our single wires across sessions was significantly smaller than variance expected from the assumption that a neuron is lost and a second neuron is gained across days (left vs. center), and from the assumption that a neuron is lost and a new neuron is recorded every day (left vs. right).

sessions ($F_{3,786} = 1.6$, $P > 0.05$, N.S.), nor was there a session × subregion interaction ($F_{3,786} = 1.3$, $P > 0.05$, N.S.). These results demonstrate that cocaine self-administration did not change on-drug baseline FRs over sessions (Figs 5B and D and 6B and D). This result is important for interpreting the change scores which will follow, as it demonstrates that longitudinal changes in response-related firing are not due to changes in baseline FR over sessions. Thus, any observed effects relate to changes in neural processing of matched head movement responses during cocaine self-administration.

Modeling of response-related FR

Visualisation of population dynamics was accomplished by plotting heat maps of response change scores across sessions for all neurons (Figs 5 and 6). Response-related firing patterns differed based on the type of neuron recorded and session (recording session × neuron type interaction – $F_{3,746} = 2.56$, $P < 0.05$; Fig. 7). *Post hoc* comparisons were conducted on the linear trends for the population of Uncategorised, Head Movement, Core, and Shell neurons in order to compare change scores at each session to a value of zero, representing 'no change' from baseline FR. Results of comparing response-related to baseline FR demonstrated that FRs of Head Movement neurons were significantly increased relative to baseline during all sessions (all $t_{746} > 2.43$, $P < 0.05$; Figs 5A and 7), while Uncategorised neurons' FRs were significantly reduced relative to baseline during all sessions (all $t_{746} < -2.78$, $P < 0.01$; Figs 5C and 7). FRs of neurons in the NAc Shell were also significantly decreased relative to baseline during all sessions (all $t_{746} < -2.57$, $P < 0.01$; Figs 6C and 7). FRs of cells in the NAc Core were reduced relative to baseline during training days 1–18 (recording sessions 1–9 – all $t_{746} < -2.86$, $P < 0.05$; Fig. 7), but were not significantly reduced relative to baseline on the remaining sessions (recording sessions 10–12 – all $t_{746} > -2.06$, $P > 0.05$, N.S.; Fig. 7). Graphical analyses of heat maps representing the population trend revealed that the shift in Core FR toward 'no change' was due entirely to individual neurons in the Core losing their inhibition during the response, not because some neurons were gaining excitation (Figs 6A and 7 inset).

Planned *post hoc* comparisons were conducted in order to make pairwise comparisons between Uncategorised, Head Movement, Core and Shell neurons across recording sessions. *Post hoc* comparisons

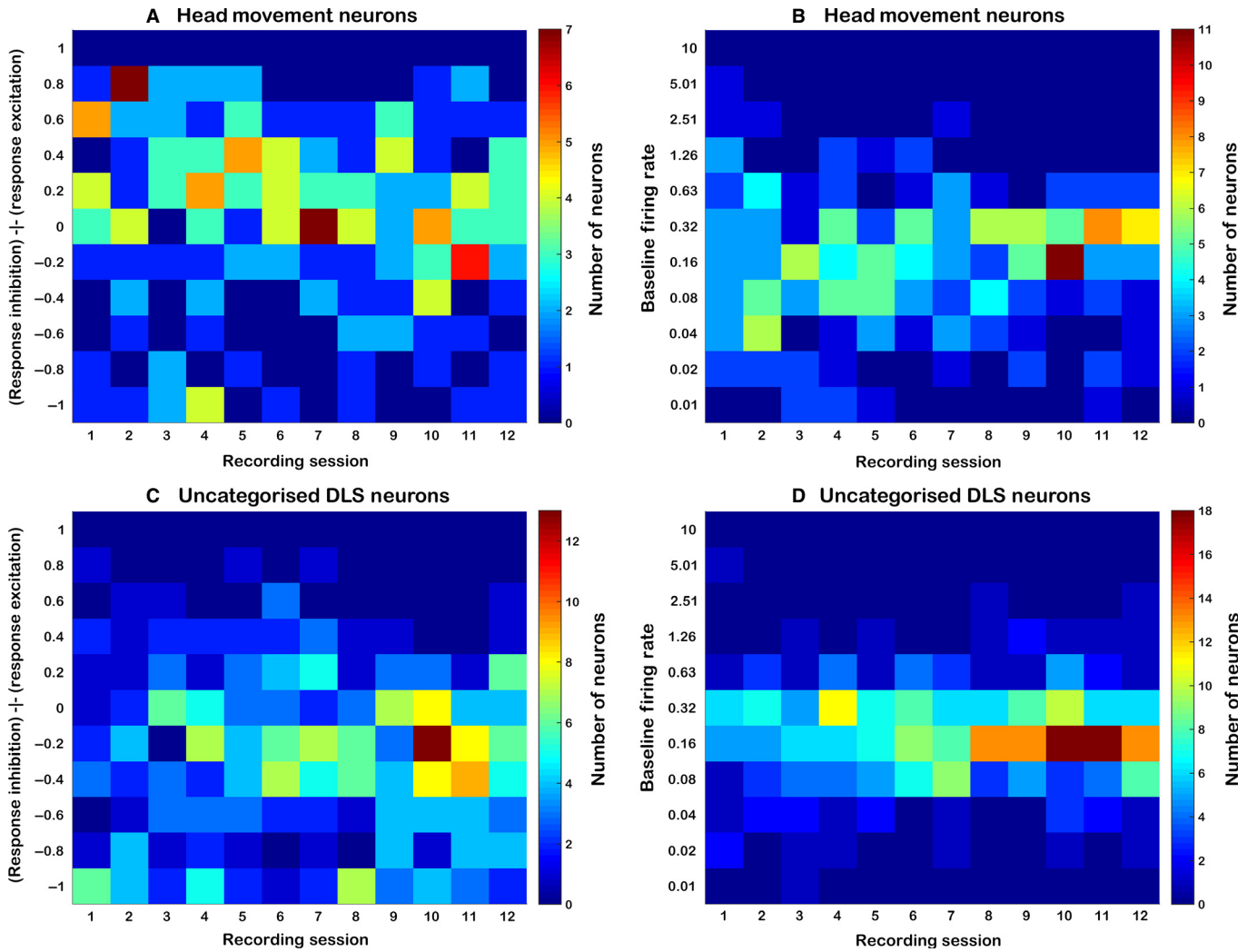

FIG. 5. Population level visualisation of DLS neuron activity. (A) Heat map containing the number of DLS Head Movement neurons falling into each category of response modulation during the operant [(Response FR − Baseline FR)/(Response FR + Baseline FR)] across sessions. Values greater than zero represent response excitation, while values below zero represent response inhibition. (B) Heat map containing baseline FRs (spikes/second) for all DLS Head Movement neurons across sessions. (C) Heat map containing the number of DLS Uncategorised neurons falling into each category of response modulation during the operant. (D) Baseline FRs for all DLS Uncategorised neurons across sessions.

showed that FRs of DLS Head Movement neurons were significantly greater than those of Uncategorised neurons during the response. This effect was present across all recording sessions (all $t_{746} > 4.14$, $P < 0.001$; Figs 5A and C and 7). Likewise, the response FRs of DLS Head Movement neurons were significantly greater than those of neurons in the NAc Core and Shell across all sessions (all $t_{746} > 3.27$, $P < 0.01$; Fig. 7). In contrast, no differences were observed in the response FRs of NAc Core and Shell neurons on any session (all $t_{746} < 1.9$, $P > 0.05$, N.S.). Similarly, the response FRs of NAc neurons did not significantly differ from those observed in Uncategorised DLS neurons (all $t_{746} < 2.4$, $P > 0.05$, N.S.).

Examples of response-related individual neuron dynamics

Head Movement neurons in the DLS receive strong excitatory input from sensory and motor cortical neurons that process head and neck activity. This excitatory cortical input was probably responsible for the increase above baseline FR in the population of DLS Head Movement neurons during operant responses across all 12 recording sessions (24 days). Some individual neurons in DLS followed this trend, showing excitation during movement from the earliest recording session until their very last (Fig. 8B). However, not all Head Movement neurons were excited during the head movement operant response on every session. Some individual Head Movement neurons were excited during the response early in training and lost that excitation across the 24 days of self-administration (Fig. 8A). Still other neurons were weakly excited during responses early in training and became progressively more excited across self-administration sessions (Fig. 8C).

As a population, NAc neurons were primarily inhibited during operant responses. For Core neurons, this inhibition could be potent, starting just before each response and extending just beyond it (Fig. 9A). The strength of this inhibition waned across self-administration sessions (Fig. 9A). Still, not all neurons in the NAc Core were inhibited during the operant response and some showed no clear or consistent pattern across sessions (Fig. 9B). The population level decrease in response inhibition in Core was not due to some neurons gaining excitation across sessions. All neurons that changed response modulation trended from highly inhibited to less inhibited

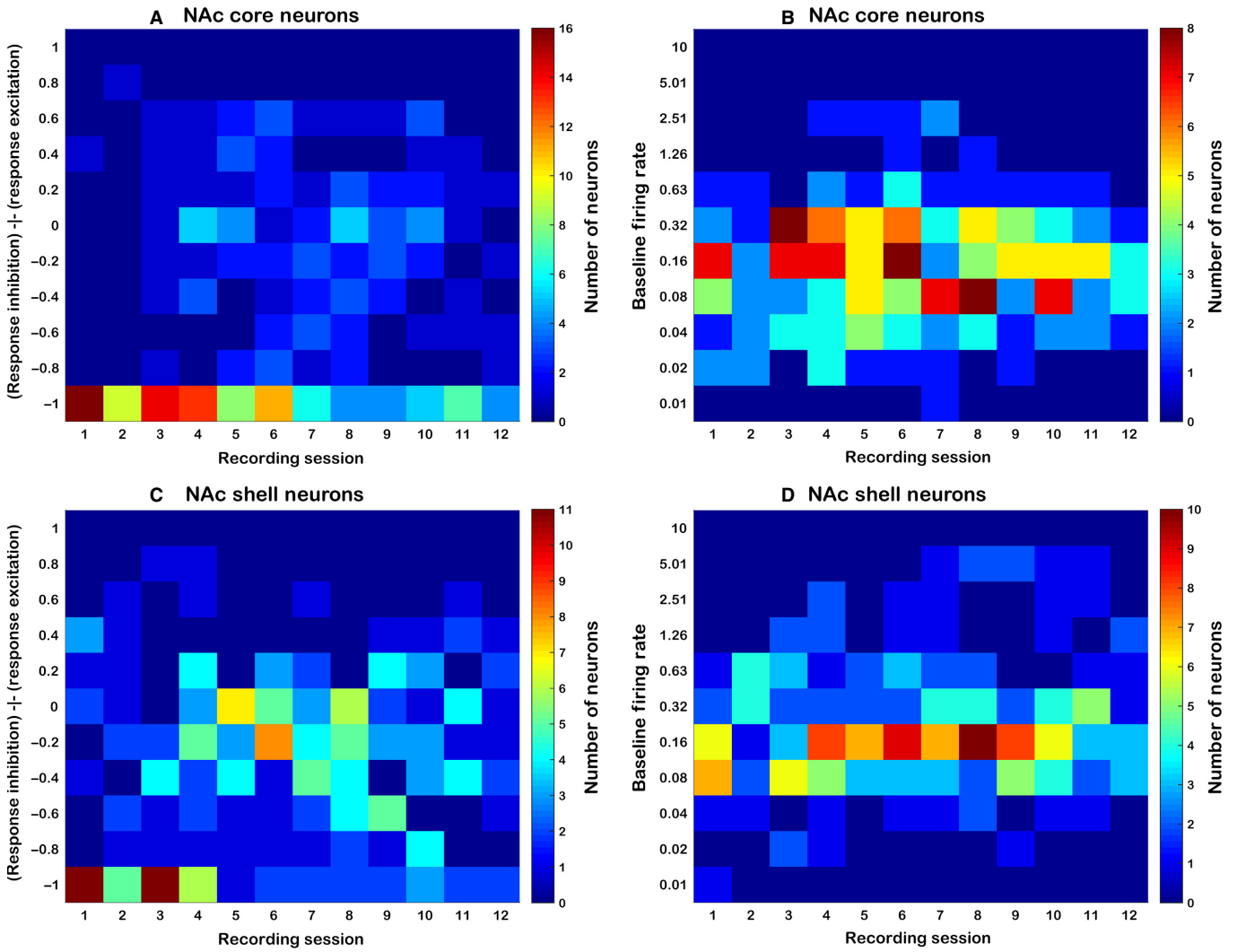

FIG. 6. Population level visualisation of NAc neuron activity. (A) Heat map containing the number of NAc Core neurons falling into each category of response modulation during the operant [(Response FR − Baseline FR)/(Response FR + Baseline FR)] across sessions. Values greater than zero represent response excitation, while values below zero represent response inhibition. (B) Heat map containing baseline FRs for all NAc Core neurons across sessions. (C) Heat map containing the number of NAc Shell neurons falling into each category of response modulation during the operant response. (D) Baseline FRs for all NAc Shell neurons across sessions.

across self-administration sessions (Fig. 7 inset). In the NAc Shell, neurons were primarily inhibited during the response and population activity remained relatively stable across all sessions. However, some individual Shell neurons did not show consistent inhibition across self-administration sessions and instead appeared to fire independently of the response (Fig. 9D).

Discussion

The key findings from the present study were that the response-related firing patterns of NAc Core neurons are modulated across protracted drug use during the specific time frame of the operant response. In contrast, firing patterns in the DLS that exhibited sensorimotor correlates specific to vertical head movements showed stable excitatory response-related FRs across protracted drug use. Similarly, NAc Shell neurons and Uncategorised (i.e., not explicitly sensorimotor responsive) neurons in the DLS were generally inhibited during the operant response and remained stable across training.

The NAc and operant responding

The present data illustrate that NAc Core neurons exhibit strong phasic inhibition during the operant response (duration typically < 0.5 s) early in training, but that these phasic response correlates become blunted across sessions. When compared to the NAc Shell, where response correlates remained stable throughout training, this important difference is probably illustrative of distinct functional processing within the NAc Core.

Dynamic changes in the firing patterns of NAc Core are likely to play a role in persistent responding during cocaine self-administration. Recent evidence demonstrated that response-related dopaminergic signaling in the NAc Core (but not the DLS) becomes attenuated across 3 weeks of repeated long-access drug use (Willuhn *et al.*, 2014). Demonstrated similarly here, response-related firing changes in the NAc Core (but not the DLS) became attenuated across 24 sessions of long access self-administration. Furthermore, the decrease in phasic dopamine signaling reported by Willuhn *et al.* was correlated with increased responding and escalation of cocaine intake. While the pres-

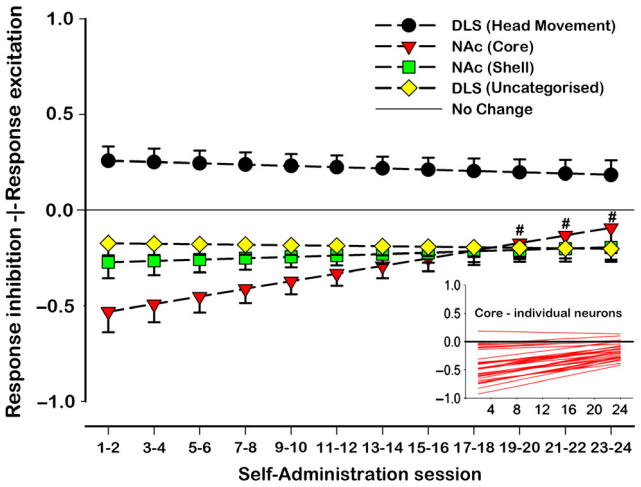

FIG. 7. Model of phasic neuronal activity during operant response. Neuronal modulation during operant movements was operationalised using the change score [(response FR − baseline FR)/(response FR + baseline FR)]. Response and baseline FRs were behaviorally matched across sessions. Core, Shell, DLS Head Movement and DLS Uncategorised neurons' firing patterns changed differentially in relation to baseline across recording sessions (recording session × neuron type interaction – $F_{3,746} = 2.56$, $P < 0.05$). DLS Head Movement neurons exhibited significantly increased FRs during matched head movements on all sessions (all $t_{746} > 2.43$, $P < 0.05$). DLS Uncategorised neurons were significantly inhibited during matched movements when compared to baseline during all sessions (all $t_{746} < -2.78$, $P < 0.01$). Neurons in the NAc Shell were also significantly decreased during all sessions when compared to baseline FRs (all $t_{746} < -2.57$, $P < 0.01$). Neurons in the NAc Core were also significantly inhibited when compared to baseline during sessions 1–18 (recording sessions 1–9 – all $t_{746} < -2.86$, $P < 0.05$), but were not significantly different from baseline during sessions 19–24 (recording sessions 10–12 – all $t_{746} > -2.06$, $P > 0.05$ N.S.) orderly, consistent loss of inhibition during response by core neurons (each line = one neuron).

ent study did not use established escalation procedures (Ahmed & Koob, 1998), animals did significantly increase drug intake through the first eight sessions and self-administered cocaine for an amount of time similar to the time of the animals of Willuhn *et al.* It is possible that during long-access self-administration, attenuation of phasic dopaminergic signaling may play a role in the attenuation of response-related inhibitions in the NAc Core.

While response-related firing patterns of NAc Shell neurons were stable over repeated drug use, their potential role in drug self-administration behavior should not be overlooked. Previous work in our laboratory has demonstrated that slow phasic progressive reversal firing patterns, which correlate with the animal's temporal spacing of self-infusions (Peoples & West, 1996), are particularly prominent in the medial NAc Shell (Fabbricatore *et al.*, 2010). Thus, by way of sensitivity to minute-to-minute fluctuations in brain cocaine concentration, the NAc Shell may be poised to drive continued drug-taking behavior via downstream influences of its phasic and slow-phasic firing patterns.

The DLS and responding

Neurons in the DLS, or sensorimotor striatum, that were related specifically to stimulation of the head and neck prior to training continued to fire phasically during vertical head movements without fluctuation throughout protracted self-administration. In the present study, the observed stability in phasic FR of DLS Head Movement neurons, which meet criteria of Type IIb striatal projection neurons (Kimura *et al.*, 1990), departs considerably from previous longitudinal studies using natural reinforcers. In those studies, DLS movement-related neurons gradually lost their response-related firing patterns and only a small minority maintained their phasic firing across operant training (Carelli *et al.*, 1997; Tang *et al.*, 2007, 2009). Thus, the maintenance of unabated sensorimotor firing during chronic cocaine self-administration probably represents an important difference in on-drug striatal processing as compared to processing natural rewards. This finding suggests that the pharmacological dose-dependent enhancement of most striatal FR in response to acute cocaine (Pederson *et al.*, 1997; Tang *et al.*, 2008; Pawlak *et al.*, 2010) or amphetamine (Ma *et al.*, 2013) is a response that persists throughout repeated exposure.

Uncategorised neurons in the DLS were unresponsive during sensorimotor examination prior to training yet exhibited slight inhibitions during operant responses as compared to their baseline FR. While the role of these neurons remains unclear, the notable difference in response pattern between these and Head Movement neurons (both presumed medium spiny neurons) emphasises the importance of considering sensorimotor correlates in studies of DLS function. A number of possibilities for the differences between Uncategorised and Head Movement neurons observed here should be considered. First, given that Uncategorised neurons were often intermixed with Head Movement neurons and demonstrated slight inhibitions during operant head movements, these neurons may be laterally inhibited by neurons related to movements of the head and neck. Second, Uncategorised neurons may have receptive zones (Prokopenko *et al.*, 2004) that are difficult to manipulate or isolate during body examinations. This would include relations with core musculature, broad muscle groups or internal muscles of the head and neck (e.g., laryngeal musculature).

It is important to note that stimulants produce stereotypical head-bobbing in rodents. However, such head movements were systematically excluded so as not to interfere with the present analyses. Specifically, baseline activity was measured during moments when the animal was completely still (no vertical or horizontal movement). Further, the operant head movements in this task were performed in a distinct location, and were quantifiably separate from stereotypical head movements (Root *et al.*, 2013). Therefore, both the baseline and response periods were devoid of stereotypical head movement.

The importance of longitudinal recordings of single-unit activity

Drug abuse is an acquired condition with a gradual behavioral onset. Accordingly, it has become a priority to track neural changes which may lead to addiction across self-administration sessions. Pioneering studies of NAc and DLS show decreased glucose utilisation from initial to chronic cocaine exposure (Macey *et al.*, 2004; Porrino *et al.*, 2004), an increase in DAT binding from initial to chronic cocaine exposure (Letchworth *et al.*, 2001), and an increase in D1 receptor binding but a decrease in D2 receptor binding from initial to chronic cocaine exposure (Nader *et al.*, 2002). In all these studies, changes in the NAc preceded those in the DLS, consistent with a shifting influence of chronic cocaine administration to more dorsal and lateral regions of striatum. These studies constitute an important step in recognising that drugs of abuse sequentially alter the striatum. Despite technical differences from measures of Porrino *et al.*, we also observed what amounts to a relative shift from ventral to dorsal striatum across sessions, in that response-related NAc Core activity declined while DLS Head Movement neuronal activity, expected to decline based on previous studies using natural rewards, remained elevated after extended training. The aforementioned studies also agree with the general decline in tonic FR observed in a study that focused only on NAc neurons across 2 weeks of cocaine

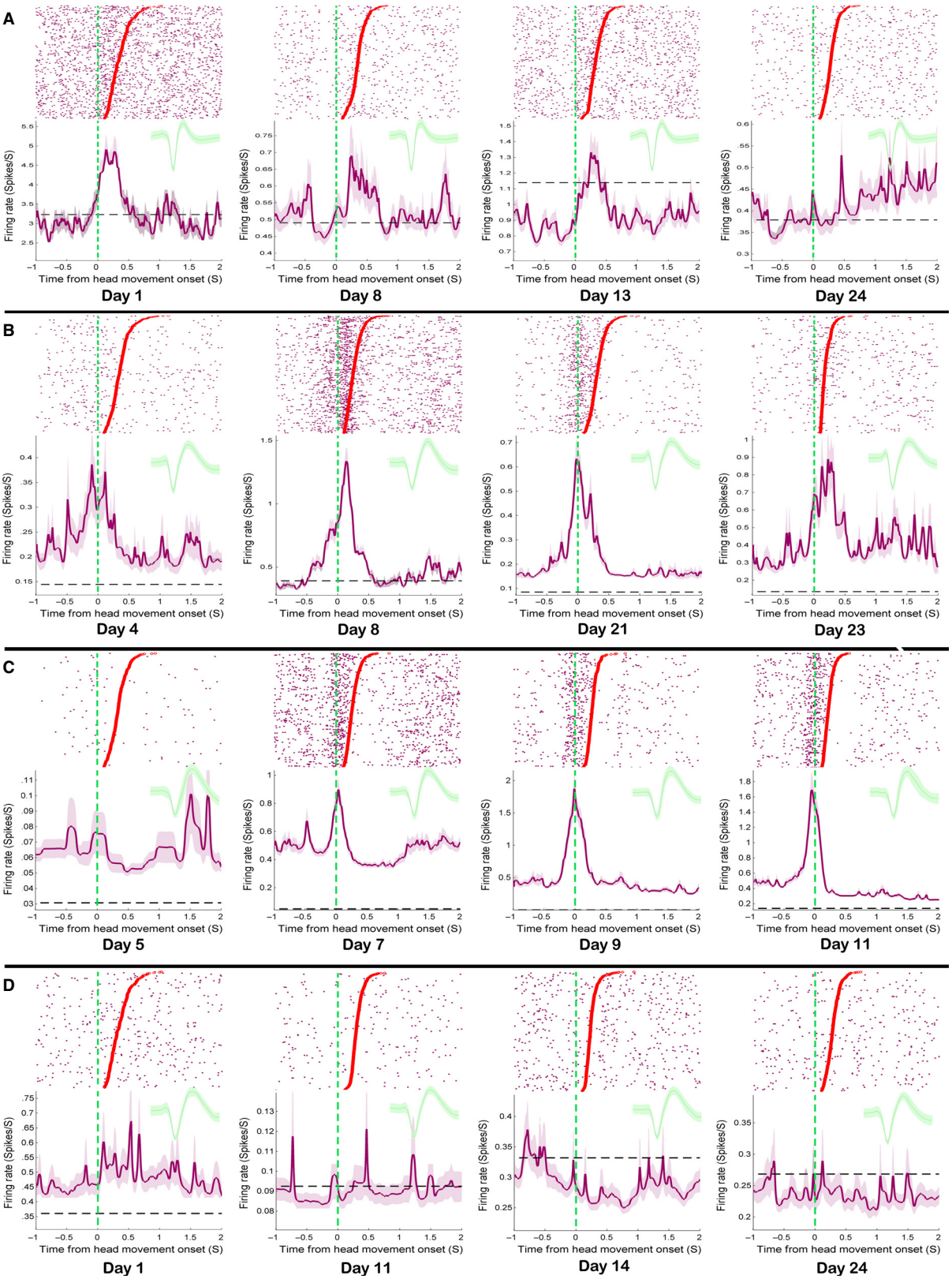

FIG. 8. Examples of DLS response related firing patterns tracked across sessions. Each row A–D shows rasters and peri-response histograms for a single neuron across sessions, as well as the mean waveform recorded during each session. Each row of the raster shows action potentials (purple dots) during a single movement. The onset of each movement is aligned to time zero, movement durations are sorted in descending order, and the offset of each individual movement is displayed as a dot. Shaded lines in each histogram show response-related FRs, while the dashed black lines show baseline FRs. (A) Some Head Movement neurons were highly excited by responses early in training and lost that activity across sessions. (B) Some remained stable throughout training, while still other (C) Head Movement neurons' response excitation became progressively more robust across sessions. (D) Uncategorised neurons in this study showed primarily mild inhibitions during the head movement response.

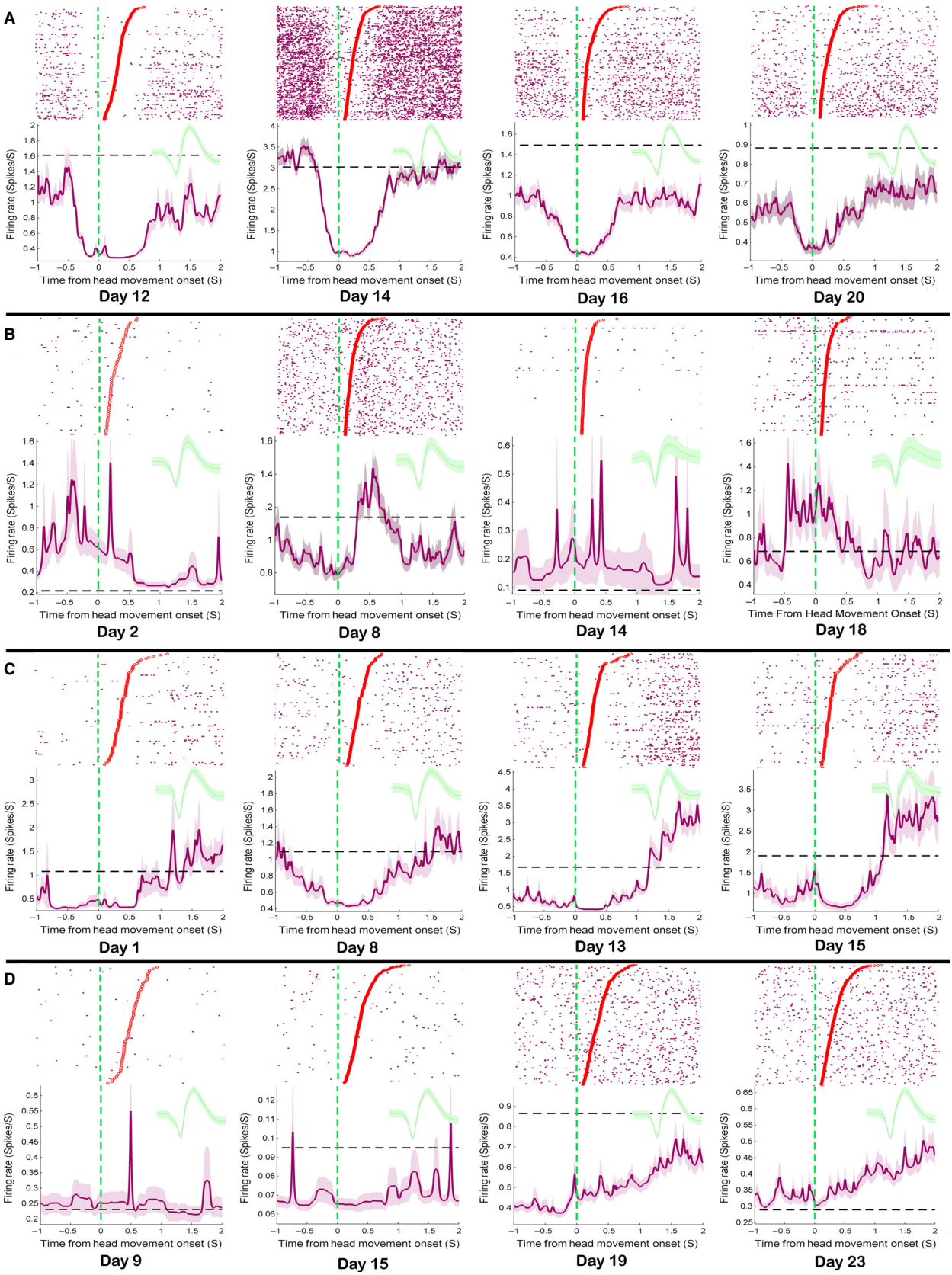

FIG. 9. Examples of NAc response related firing patterns tracked across sessions. Each row A–D shows rasters and peri-response histograms for a single neuron across sessions, as well as the mean waveform recorded during each session. Details are the same as Fig. 8. (A) Most Core neurons were inhibited strongly during response early in training and lost that inhibition by late sessions. (B) However, not all Core neurons were consistently inhibited during the response. (C) Shell neurons were also inhibited during response and some maintained that inhibition throughout training. (D) However, not all shell neurons were consistently inhibited during the response.

self-administration (Peoples *et al.*, 1999). While the present study did not reveal similar changes in baseline FR (probably owing to differences from the study by Peoples *et al.* in controls for movement, drug dose, drug level, etc.), it sought to extend this line of work to focus on phasic, response-related, changes in both the NAc and DLS. Single-unit recordings represent one of only a few recognised methods for tracking phasic changes in individual neuron activity over time, and allow for subregional specificity on millisecond time scales (Thompson & Best, 1990; Carelli *et al.*, 1997; Greenberg & Wilson, 2004; Schmitzer-Torbert & Redish, 2004; Jackson & Fetz, 2007; Tang *et al.*, 2007, 2009; Tolias *et al.*, 2007; Dickey *et al.*, 2009; Fraser & Schwartz, 2012; Lütcke *et al.*, 2013; McMahon *et al.*, 2014).

The present first-of-its-kind study demonstrates diverse roles for specific subregions of the striatum in drug-taking behaviors. The data suggest that all striatal subregions show changes in FR during the brief time frame of the operant response, but a number of important differences in the way these regions process response-related firing demonstrate that drug-related processing is both subregionally specific and dependent on the somatic sensorimotor properties of the recorded neuron. While response-related firing patterns were observed in both NAc and DLS, somatotopically organised processing of single body parts was detected only in DLS during body examinations. This suggests both that the primary role of DLS neurons is somatic sensorimotor and that NAc neurons may be processing information during the response that is not explicitly sensorimotor. Whereas DLS Type IIb neurons process the self-administering response, they do not explicitly process cues related to reward (Root *et al.*, 2010). Processing of a cocaine cue has been observed in the NAc Shell (Ghitza *et al.*, 2003) during reinstatement. Most importantly, longitudinal changes in response correlates were observed only in the NAc Core, suggesting that this region is particularly susceptible to plastic changes in response-related firing induced by abused drugs. Nevertheless, the fact that the NAc Shell, NAc Core and DLS all exhibit phasic changes in FR during the operant response is consistent with anatomical evidence that serial, multisynaptic processing may occur within the striatum (Haber *et al.*, 2000).

Conflict of interests

The authors declare no competing financial interests

Acknowledgements

We thank Carla Ralston, Brendan Striano, Olivia Kim, Thomas Grace Sr., and Jackie Thomas for excellent assistance. This study was supported by the National Institute on Drug Abuse Grants DA006886 (MOW) and DA032270 (DJB). All coauthors have seen and approve of the contents of the manuscript.

Abbreviations

DLS, dorsolateral striatum; FI, fixed interval; FR, firing rate; ISI, inter spike interval; NAc, nucleus accumbens; VI, variable interval.

References

Ahmed, S.H. & Koob, G.F. (1998) Transition from moderate to excessive drug intake: change in hedonic set point. *Science*, **282**, 298–300.

Alexander, G.E. & DeLong, M.R. (1985) Microstimulation of the primate neostriatum. II. Somatotopic organization of striatal microexcitable zones and their relation to neuronal response properties. *J. Neurophysiol.*, **53**, 1417–1430.

Alexander, G.E., DeLong, M.R. & Strick, P.L. (1986) Parallel organization of functionally segregated circuits linking basal ganglia and cortex. *Annu. Rev. Neurosci.*, **9**, 357–381.

Barker, D.J., Bercovicz, D., Servilio, L.C., Simmons, S.J., Ma, S., Root, D.H., Pawlak, A.P. & West, M.O. (2014) Rat ultrasonic vocalizations demonstrate that the motivation to contextually reinstate cocaine-seeking behavior does not necessarily involve a hedonic response. *Addict. Biol.*, **19**, 781–790.

Belin, D. & Everitt, B.J. (2008) Cocaine seeking habits depend upon dopamine-dependent serial connectivity linking the ventral with the dorsal striatum. *Neuron*, **57**, 432–441.

Brog, J.S., Salyapongse, A., Deutch, A.Y. & Zahm, D.S. (1993) The patterns of afferent innervation of the core and shell in the "accumbens" part of the rat ventral striatum: immunohistochemical detection of retrogradely transported fluoro-gold. *J. Comp. Neurol.*, **338**, 255–278.

Brown, L.L. (1992) Somatotopic organization in rat striatum: evidence for a combinational map. *Proc. Natl. Acad. Sci. USA*, **89**, 7403–7407.

Brown, L.L. & Sharp, F.R. (1995) Metabolic mapping of rat striatum: somatotopic organization of sensorimotor activity. *Brain Res.*, **686**, 207–222.

Brown, L.L., Smith, D.M. & Goldbloom, L.M. (1998) Organizing principles of cortical integration in the rat neostriatum: corticostriate map of the body surface is an ordered lattice of curved laminae and radial points. *J. Comp. Neurol.*, **392**, 468–488.

Carelli, R.M. & West, M.O. (1991) Representation of the body by single neurons in the dorsolateral striatum of the awake, unrestrained rat. *J. Comp. Neurol.*, **309**, 231–249.

Carelli, R.M., Wolske, M. & West, M.O. (1997) Loss of lever press-related firing of rat striatal forelimb neurons after repeated sessions in a lever pressing task. *J. Neurosci.*, **17**, 1804–1814.

Cho, J. & West, M.O. (1997) Distribution of single neurons related to body parts in the lateral striatum of the rat. *Brain Res.*, **756**, 241–246.

Coffey, K.R., Barker, D.J., Ma, S. & West, M.O. (2013) Building an open-source robotic stereotaxic instrument. *J. Vis. Exp.*, e51006.

Crutcher, M.D. & Delong, M.R. (1984) Single cell studies of the primate putamen. I. Functional organization. *Exp. Brain Res.*, **53**, 233–243.

Dickey, A.S., Suminski, A., Amit, Y. & Hatsopoulos, N.G. (2009) Single-unit stability using chronically implanted multielectrode arrays. *J. Neurophysiol.*, **102**, 1331–1339.

Fabbricatore, A.T., Ghitza, U.E., Prokopenko, V.F. & West, M.O. (2010) Electrophysiological evidence of mediolateral functional dichotomy in the rat nucleus accumbens during cocaine self-administration II: phasic firing patterns. *Eur. J. Neurosci.*, **31**, 1671–1682.

Feltenstein, M.W. & See, R.E. (2008) The neurocircuitry of addiction: an overview. *Brit. J. Pharmacol.*, **154**, 261–274.

François, C., Yelnik, J. & Percheron, G. (1994) Calbindin D-28k as a marker for the associative cortical territory of the striatum in macaque. *Brain Res.*, **633**, 331–336.

Fraser, G.W. & Schwartz, A.B. (2012) Recording from the same neurons chronically in motor cortex. *J. Neurophysiol.*, **107**, 1970–1978.

Fudge, J.L. & Haber, S.N. (2002) Defining the caudal ventral striatum in primates: cellular and histochemical features. *J. Neurosci.*, **22**, 10078–10082.

Gerdeman, G.L., Partridge, J.G., Lupica, C.R. & Lovinger, D.M. (2003) It could be habit forming: drugs of abuse and striatal synaptic plasticity. *Trends Neurosci.*, **26**, 184–192.

Ghitza, U.E., Fabbricatore, A.T., Prokopenko, V., Pawlak, A.P. & West, M.O. (2003) Persistent cue-evoked activity of accumbens neurons after prolonged abstinence from self-administered cocaine. *J. Neurosci.*, **23**, 7239–7245.

Greenberg, P.A. & Wilson, F.A. (2004) Functional stability of dorsolateral prefrontal neurons. *J. Neurophysiol.*, **92**, 1042–1055.

Haber, S.N., Fudge, J.L. & McFarland, N.R. (2000) Striatonigrostriatal pathways in primates form an ascending spiral from the shell to the dorsolateral striatum. *J. Neurosci.*, **20**, 2369–2382.

Hanlon, C.A., Wesley, M.J. & Porrino, L.J. (2009) Loss of functional specificity in the dorsal striatum of chronic cocaine users. *Drug Alcohol Depen.*, **102**, 88–94.

Institute of Laboratory Animal Resources (US). Committee on Care, Use of Laboratory Animals, & National Institutes of Health (US). Division of Research Resources (1985) *Guide for the Care and use of Laboratory Animals*. National Academies, Washington, DC.

Jackson, A. & Fetz, E.E. (2007) Compact movable microwire array for long-term chronic unit recording in cerebral cortex of primates. *J. Neurophysiol.*, **98**, 3109–3118.

Kimura, M., Kato, M. & Shimazaki, H. (1990) Physiological properties of projection neurons in the monkey striatum to the globus pallidus. *Exp. Brain Res.*, **82**, 672–676.
Kosobud, A.E., Harris, G.C. & Chapin, J.K. (1994) Behavioral associations of neuronal activity in the ventral tegmental area of the rat. *J. Neurosci.*, **14**, 7117–7129.
Letchworth, S.R., Nader, M.A., Smith, H.R., Friedman, D.P. & Porrino, L.J. (2001) Progression of changes in dopamine transporter binding site density as a result of cocaine self-administration in rhesus monkeys. *J. Neurosci.*, **21**, 2799–2807.
Liles, S.L. & Updyke, B.V. (1985) Projection of the digit and wrist area of precentral gyrus to the putamen: relation between topography and physiological properties of neurons in the putamen. *Brain Res.*, **339**, 245–255.
Lütcke, H., Margolis, D.J. & Helmchen, F. (2013) Steady or changing? Long-term monitoring of neuronal population activity. *Trends Neurosci.*, **36**, 375–384.
Macey, D.J., Rice, W.N., Freedland, C.S., Whitlow, C.T. & Porrino, L.J. (2004) Patterns of functional activity associated with cocaine self-administration in the rat change over time. *Psychopharmacology*, **172**, 384–392.
Ma, S., Pawlak, A.P., Cho, J., Root, D.H., Barker, D.J. & West, M.O. (2013) Amphetamine's dose-dependent effects on dorsolateral striatum sensorimotor neuron firing. *Behav. Brain Res.*, **244**, 152–161.
Marchant, N.J., Li, X. & Shaham, Y. (2013) Recent developments in animal models of drug relapse. *Curr. Opin. Neurobiol.*, **23**, 675–683.
McMahon, D.B., Bondar, I.V., Afuwape, O.A., Ide, D.C. & Leopold, D.A. (2014) One month in the life of a neuron: longitudinal single-unit electrophysiology in the monkey visual system. *J. Neurophysiol.*, **112**, 1748–1762.
Meredith, G.E., Pattiselanno, A., Groenewegen, H.J. & Haber, S.N. (1996) Shell and core in monkey and human nucleus accumbens identified with antibodies to calbindin-D28k. *J. Comp. Neurol.*, **365**, 628–639.
Mittler, T., Cho, J., People, L.L. & West, M.O. (1994) Representation of the body in the lateral striatum of the freely moving rat: single neurons related to licking. *Exp. Brain Res.*, **98**, 163–167.
Nader, M.A., Daunais, J.B., Moore, T., Nader, S.H., Moore, R.J., Smith, H.R., Friedman, D.P. & Porrino, L.J. (2002) Effects of cocaine self-administration on striatal dopamine systems in rhesus monkeys: initial and chronic exposure. *Neuropsychopharmacology*, **27**, 35–46.
Nauta, W.J., Smith, G.P., Faull, R.L.M. & Domesick, V.B. (1978) Efferent connections and nigral afferents of the nucleus accumbens septi in the rat. *Neuroscience*, **3**, 385–401.
Parent, A. (1990) Extrinsic connections of the basal ganglia. *Trends Neurosci.*, **13**, 254–258.
Pawlak, A., Tang, C., Pederson, C.L., Wolske, M. & West, M.O. (2010) Acute effects of cocaine on movement-related firing of dorsolateral striatal neurons depend on baseline firing rate and dose. *J. Pharmacol. Exp. Ther.*, **332**, 667–683.
Pederson, C.L., Wolske, M., Peoples, L.L. & West, M.O. (1997) Firing rate dependent effect of cocaine on single neurons of the rat lateral striatum. *Brain Res.*, **760**, 261–265.
Peoples, L.L. & West, M.O. (1996) Phasic firing of single neurons in the rat nucleus accumbens correlated with the timing of intravenous cocaine self-administration. *J. Neurosci.*, **16**, 3459–3473.
Peoples, L.L., Uzwiak, A.J., Gee, F. & West, M.O. (1999) Tonic firing of rat nucleus accumbens neurons: changes during the first 2 weeks of daily cocaine self-administration sessions. *Brain Res.*, **822**, 231–236.
Porrino, L.J. (1993) Functional consequences of acute cocaine treatment depend on route of administration. *Psychopharmacology*, **112**, 343–351.
Porrino, L.J., Lyons, D., Smith, H.R., Daunais, J.B. & Nader, M.A. (2004) Cocaine self-administration produces a progressive involvement of limbic, association, and sensorimotor striatal domains. *J. Neurosci.*, **24**, 3554–3562.
Prokopenko, V.F., Pawlak, A. & West, M.O. (2004) Fluctuations in somatosensory responses and baseline firing rates of neurons in the lateral striatum of freely moving rats: effects of intranigral apomorphine. *J. Neurosci.*, **125**, 1077–1082.
Rall, W. (1962) Electrophysiology of a dendritic neuron model. *Biophys. J.*, **2**, 145.
Raudenbush, S.W. & Bryk, A.S. (2002) *Hierarchical Linear models: Applications and Data Analysis Methods*, 2nd Edn. Sage Publications, Thousand Oaks, CA.
Robbins, T.W. & Everitt, B.J. (2002) Limbic-striatal memory systems and drug addiction. *Neurobiol. Learn. Mem.*, **78**, 625–636.
Root, D.H., Fabbricatore, A.T., Barker, D.J., Ma, S., Pawlak, A.P. & West, M.O. (2009) Evidence for habitual and goal-directed behavior following devaluation of cocaine: a multifaceted interpretation of relapse. *PLoS One*, **4**, e7170.
Root, D.H., Tang, C.C., Ma, S., Pawlak, A.P. & West, M.O. (2010) Absence of cue-evoked firing in rat dorsolateral striatum neurons. *Behav. Brain Res.*, **211**, 23–32.
Root, D.H., Ma, S., Barker, D.J., Megehee, L., Striano, B.M., Ralston, C.M., Fabbricatore, A.T. & West, M.O. (2013) Differential roles of ventral pallidum subregions during cocaine self-administration behaviors. *J. Comp. Neurol.*, **521**, 558–588.
Schmitzer-Torbert, N. & Redish, A.D. (2004) Neuronal activity in the rodent dorsal striatum in sequential navigation: separation of spatial and reward responses on the multiple T task. *J. Neurophysiol.*, **91**, 2259–2272.
Schmitzer-Torbert, N., Jackson, J., Henze, D., Harris, K. & Redish, A.D. (2005) Quantitative measures of cluster quality for use in extracellular recordings. *Neuroscience*, **131**, 1–11.
Tang, C., Pawlak, A.P., Prokopenko, V.F. & West, M.O. (2007) Changes in activity of the striatum during formation of a motor habit. *Eur. J. Neurosci.*, **25**, 1212–1227.
Tang, C., Mittler, T., Duke, D.C., Zhu, Y., Pawlak, A.P. & West, M.O. (2008) Dose-and rate-dependent effects of cocaine on striatal firing related to licking. *J. Pharmacol. Exp. Ther.*, **324**, 701–713.
Tang, C.C., Root, D.H., Duke, D.C., Zhu, Y., Teixeria, K., Ma, S., Barker, D.J. & West, M.O. (2009) Decreased firing of striatal neurons related to licking during acquisition and overtraining of a licking task. *J. Neurosci.*, **29**, 13952–13961.
Thomas, M.J., Kalivas, P.W. & Shaham, Y. (2008) Neuroplasticity in the mesolimbic dopamine system and cocaine addiction. *Brit. J. Pharmacol.*, **154**, 327–342.
Thompson, L.T. & Best, P.J. (1990) Long-term stability of the place-field activity of single units recorded from the dorsal hippocampus of freely behaving rats. *Brain Res.*, **509**, 299–308.
Tiffany, S.T. (1990) A cognitive model of drug urges and drug-use behavior: role of automatic and nonautomatic processes. *Psychol. Rev.*, **97**, 147.
Tolias, A.S., Ecker, A.S., Siapas, A.G., Hoenselaar, A., Keliris, G.A. & Logothetis, N.K. (2007) Recording chronically from the same neurons in awake, behaving primates. *J. Neurophysiol.*, **98**, 3780–3790.
Usuda, I., Tanaka, K. & Chiba, T. (1998) Efferent projections of the nucleus accumbens in the rat with special reference to subdivision of the nucleus: biotinylated dextran amine study. *Brain Res.*, **797**, 73–93.
Volkow, N.D., Wang, G.J., Telang, F., Fowler, J.S., Logan, J., Childress, A.R., Jayne, M., Ma, Y. & Wong, C. (2006) Cocaine cues and dopamine in dorsal striatum: mechanism of craving in cocaine addiction. *J. Neurosci.*, **26**, 6583–6588.
West, M.O., Carelli, R.M., Cohen, S.M., Gardner, J.P., Pomerantz, M., Chapin, J.K. & Woodward, D.J. (1990) A region in the dorsolateral striatum of the rat exhibiting single unit correlations with specific locomotor limb movements. *J. Neurophysiol.*, **64**, 690–703.
Willuhn, I., Burgeno, L.M., Groblewski, P.A. & Phillips, P.E. (2014) Excessive cocaine use results from decreased phasic dopamine signaling in the striatum. *Nat. Neurosci.*, **17**, 704–709.
Wright, C.I., Beijer, A.V.J. & Groenewegen, H.J. (1996) Basal amygdaloid complex afferents to the rat nucleus accumbens are compartmentally organized. *J. Neurosci.*, **16**, 1877–1893.
Zahm, D.S. & Heimer, L. (1988) Ventral striatopallidal parts of the basal ganglia in the rat: I. Neurochemical compartmentation as reflected by the distributions of neurotensin and substance p immunoreactivity. *J. Comp. Neurol.*, **272**, 516–535.
Zahm, D.S. & Heimer, L. (1990) Two transpallidal pathways originating in the rat nucleus accumbens. *J. Comp. Neurol.*, **302**, 437–446.